

On a retarded stochastic system with discrete diffusion modeling life tables

Tomás Caraballo¹, Francisco Morillas², José Valero³

¹ Universidad de Sevilla, Departamento de Ecuaciones Diferenciales y Análisis Numérico

Apdo. de Correos 1160, 41080-Sevilla Spain

E.mail: caraball@us.es

² Universitat de València, Departament d'Economia Aplicada, Facultat d'Economia,

Campus dels Tarongers s/n, 46022-València, Spain.

E.mail: Francisco.Morillas@uv.es

³ Universidad Miguel Hernández de Elche, Centro de Investigación Operativa

Avda. Universidad s/n, Elche (Alicante), 03202, Spain.

E.mail: jvalero@umh.es

Abstract

This work proposes a method for modeling and forecasting mortality rates. It constitutes an improvement over previous studies by incorporating both the historical evolution of the mortality phenomenon and its random behavior. In the first part, we introduce the model and analyze mathematical properties such as the existence of solutions and their asymptotic behavior. In the second part, we apply this model to forecast mortality rates in Spain, showing that it yields better results than classical methods.

1 Introduction

In actuarial or demographic sciences, life tables are very useful to study biometric functions such as the probability of survival or death, therefore they are crucial to calculate the insurance premium. In our previous papers [34], [35], [7], we have shown that a system of ordinary differential equations with nonlocal discrete diffusion is appropriate to model dynamical life tables. In [34], we implemented the deterministic model

$$\begin{aligned} \frac{d}{dt}u_i(t) &= \sum_{r \in D} j_{i-r}u_r(t) - u_i(t) + \sum_{r \in \mathbb{Z} \setminus D} j_{i-r}g_r(t), \quad i \in D, \quad t > 0, \\ u_i(0) &= u_i^0, \quad i \in D, \end{aligned} \quad (1)$$

where $D = \{m_1, \dots, m_2\}$, $m_1 < m_2$, $m_i \in \mathbb{Z}$, and $j : \mathbb{Z} \rightarrow \mathbb{R}^+$. Using the observed data published by Spain's National Institute of Statistics, we compared the results of our model with those obtained through classical techniques. Our numerical simulations indicate that, in the short run—specifically for predictions within three years—we achieved improvements in certain indicators of goodness and smoothness. Since some memory effects are present on life tables, we considered in [35] a modification of model (1) in which we added some delay terms. Namely, we studied the problem:

$$\begin{aligned} \frac{d}{dt}u_i(t) &= \sum_{r \in D} \int_{-h}^0 j_{i-r}u^r(t+s)\alpha_i(s)d\mu(s) - u_i(t) \\ &\quad + \sum_{r \in \mathbb{Z} \setminus D} \int_{-h}^0 j_{i-r}g_r(t+s)\alpha_i(s)d\mu(s), \quad i \in D, \quad t > 0, \\ u^i(\tau+s) &\equiv \phi^i(s), \quad i \in D, \quad s \in [-h, 0], \end{aligned} \quad (2)$$

where $\alpha_i : [-s, 0] \rightarrow \mathbb{R}^+$ and $d\mu(s) = \xi(s) ds$ being $\xi(\cdot)$ a probability density. In [35] it was shown that with this model the prediction horizon can be extended up to 8 years. In addition, it gives coherent values, in magnitude, when comparing it with other classical techniques such as the Lee-Carter model, up to 18 years.

Despite the good results provided by these deterministic models, in the real world there is always a certain level of noise, which either can be intrinsic to the model or can appear due to the presence of errors in the observed data. This is why in [7] we considered the stochastic version of model (1) given by

$$\begin{aligned} \frac{d}{dt} u_i(t) &= \sum_{r \in D} j_{i-r} u_r(t) - u_i(t) + \sum_{r \in \mathbb{Z} \setminus D} j_{i-r} g_r(t) + b \sigma_i(u_i(t)) \frac{dw_i}{dt}, \quad i \in D, t > 0, \\ u_i(0) &= u_i^0, \quad i \in D, \end{aligned} \quad (3)$$

where $w_i(t)$ are independent Brownian motions and $b > 0$ is the intensity of the white noise, and two specific type of noises were considered: 1) $\sigma_i(v) = v$ (linear case); 2) $\sigma_i(v) = v(1 - v)$. The choice of the noise in the second case is motivated by the fact that we are interested in studying variables like the probability of death, which take values in the interval $[0, 1]$. Although the results given by the numerical simulations are fine from the qualitative point of view, it was necessary to make a correction of the estimates by using the average annual improvement rate. However, this correction is not equally adequate for all ages. Thus, in order to take into account in the model appropriate correction rates for each age, we need to introduce delay terms in the equation as in (2). Therefore, we will study in this paper the following stochastic system of differential equations with delay:

$$\begin{cases} \frac{d}{dt} u^i(t) = [J(t, u_t)]_i - u^i(t) + b \sigma_i(u_i(t)) \frac{dw_i}{dt}, & i \in D, t > \tau, \\ u^i(\tau + s) \equiv \phi^i(s), & i \in D, s \in [-h, 0], \end{cases} \quad (4)$$

where $D = \{m_1, m_1 + 1, \dots, m_2\}$, $-\infty < m_1 < m_2 < \infty$, $m = m_2 - m_1 + 1$, τ is the initial moment of time, $h > 0$, $w_i(t)$ are independent Brownian motions, $b \geq 0$ is the intensity of the white noise, $\sigma_i : \mathbb{R} \rightarrow \mathbb{R}$, and $J : \mathbb{R}^+ \times C([-h, 0], \mathbb{R}^m) \rightarrow \mathbb{R}^m$ is the non-autonomous convolution operator defined by

$$[J(t, u_t)]_i = \sum_{r \in D} \int_{-h}^0 j_{i-r} u^r(t+s) \alpha_i(s) d\mu(s) + \sum_{r \in \mathbb{Z} \setminus D} \int_{-h}^0 j_{i-r} g_r(t+s) \alpha_i(s) d\mu(s), \quad \text{if } i \in D,$$

where $u(t) = (u^i(s))_{i \in D}$, u_t is the segment of solution defined by $u_t(s) = u(t+s)$ for $s \in [-h, 0]$, $j : \mathbb{Z} \rightarrow \mathbb{R}$, $g : \mathbb{R} \times \mathbb{Z} \setminus D \rightarrow \mathbb{R}$ and $d\mu(s) = \xi(s) ds$ being $\xi(\cdot)$ a probability density. We define the Banach space

$$l_2^\infty = \{(u_i)_{i \in \mathbb{Z} \setminus D} : \sup_{i \in \mathbb{Z} \setminus D} |u_i| < \infty\}$$

with the norm $\|u\|_{l_2^\infty} = \sup_{i \in \mathbb{Z} \setminus D} |u_i|$ and assume the following conditions:

(H1) $j_k \geq 0$ for all $k \in \mathbb{Z}$.

(H2) $\sum_{i \in \mathbb{Z}} j_i = 1$.

(H3) $g \in C(\mathbb{R}, l_2^\infty)$.

(H4) $\alpha_i \in C([-h, 0], \mathbb{R})$, $\alpha_i(s) \geq 0$ for $i \in D$, $s \in [-h, 0]$.

As for problem (3) we will consider the noises $\sigma_i(v) = v$ (linear case) and $\sigma_i(v) = v(1 - v)$.

In the first part of the paper, we study several properties of the solutions to problem (4). In the case where the noise is linear, we establish the existence of a unique globally defined positive solution if the initial condition is positive. When the noise is non-linear with $\sigma_i(v) = v(1 - v)$, we prove that if the initial condition belongs to $(0, 1)$, then the solution remains in this interval for any future moment of time. Finally, we analyze the asymptotic behaviour of the solutions as time goes to $+\infty$, showing under certain assumptions that, for large enough time, the solution belongs to a neighbourhood of the unique fixed point of the deterministic system.

In the second part of the paper, we apply model (4) to forecast age-specific mortality rates in Spain. Using observed data from 2008 to 2018, we perform numerical simulations to generate multiple realizations of predicted mortality values for the period 2019–2023. Based on these realizations, we construct confidence intervals and calculate several error indicators, comparing the results with those obtained from classical techniques such as the Lee-Carter and Renshaw-Haberman models. Our model achieved the best results for all years within the validation period (2019–2023). Thus, we conclude that our method should be regarded as a promising alternative to classical models.

2 Properties of solutions

In this section, we shall obtain some properties of the solutions to problem (4).

3 The linear case

We will first consider a standard linear noise, that is, we study the system

$$\begin{aligned} \frac{d}{dt}u_i(t) &= [J(t, u_t)]_i - u_i(t) + bu_i(t)\frac{dw_i}{dt}, \quad i \in D, \quad t > \tau, \\ u_i(\tau + s) &\equiv \phi^i(s), \quad i \in D, \quad s \in [-h, 0]. \end{aligned} \quad (5)$$

Denote $\mathbb{R}_+^m = \{v \in \mathbb{R}^m : v_j > 0 \text{ for all } j\}$ and $\bar{\alpha}_i = \int_{-h}^0 \alpha_i(s) d\mu(s)$. Our aim is to establish the existence of global positive solutions.

Lemma 1 *Assume that $g_r(t) \geq 0$, for all r and t , and that $\bar{\alpha}_i \leq 1$, for all i . Then for any $\phi \in C([-h, 0], \mathbb{R}_+^m)$ there exists a unique globally defined solution $u(\cdot)$ such that $u(t) \in \mathbb{R}_+^m$ almost sure for $t \geq \tau$.*

Proof. The existence of a unique local solution to problem (5) follows from standard results for functional stochastic differential equations governed by locally Lipschitz functions [31, Theorem 2.8, P. 154]. Given that any solution $u(\cdot)$ is defined in the maximal interval $[0, \tau_e)$, we need to prove that $\tau_e = +\infty$ and that $u(t) \in \mathbb{R}_+^m$ for all $t \geq 0$ a.s.

We choose $k_0 > 0$ such that

$$\frac{1}{k_0} < \min_{s \in [-h, 0]} |\phi_i(s)| \leq \max_{s \in [-h, 0]} |\phi_i(s)| < k_0 \text{ for all } i \in D.$$

For each $k \geq k_0$ we define the stopping time

$$\tau_k = \inf\{t \in [\tau, \tau_e) : u_i(t) \notin (\frac{1}{k}, k) \text{ for some } i \in D\}.$$

This sequence is increasing as $k \nearrow +\infty$. If $\tau_\infty = \lim_{k \rightarrow +\infty} \tau_k = +\infty$ a.s., then $\tau_e = +\infty$ and $u(t) \in \mathbb{R}_+^m$ for $t \geq 0$ almost surely, proving the assertion.

If $\lim_{k \rightarrow +\infty} \tau_k \neq +\infty$ a.s., there would exist $T, \varepsilon > 0$ such that

$$P(\tau_\infty \leq T) > \varepsilon,$$

and then there would be $k_1 \geq k_0$ for which

$$P(\tau_k \leq T) \geq \varepsilon \text{ for } k \geq k_1.$$

Further, we consider the C^2 -function $V : \mathbb{R}_+^m \rightarrow \mathbb{R}_+^1$ given by

$$V(u) = \sum_{i \in D} (u_i - 1 - \log(u_i)).$$

Let $\tau \leq t \leq \tau_k \wedge T$. Then $u(t) \in \mathbb{R}_+^m$ and by Itô's formula we have

$$\begin{aligned}
dV(u(t)) &= \sum_{i \in D} \left(1 - \frac{1}{u_i(t)}\right) \left(\sum_{r \in D} \int_{-h}^0 j_{i-r} u_r(t+s) \alpha_i(s) d\mu(s) + \sum_{r \in \mathbb{Z} \setminus D} \int_{-h}^0 j_{i-r} g_r(t+s) \alpha_i(s) d\mu(s) - u_i(t) \right) dt \\
&+ \sum_{i \in D} \frac{1}{2} b^2 dt + \sum_{i \in D} \left(1 - \frac{1}{u_i(t)}\right) b u_i(t) dw_i(t) \\
&= I(t) dt + \sum_{i \in D} I_i(t) dw_i(t),
\end{aligned} \tag{6}$$

where $I_i(t) = \left(1 - \frac{1}{u_i(t)}\right) b u_i(t)$. By using (H1) – (H4), $u(t) \in \mathbb{R}_+^m$ and $g_r(t) \geq 0$ the first term is estimated by:

$$\begin{aligned}
I(t) &\leq \sum_{i \in D} \sum_{r \in D} \int_{-h}^0 j_{i-r} u_r(t+s) \alpha_i(s) d\mu(s) - \sum_{i \in D} u_i(t) + m + \frac{m}{2} b^2 \\
&+ \sum_{i \in D} \sum_{r \in \mathbb{Z} \setminus D} \int_{-h}^0 j_{i-r} g_r(t+s) \alpha_i(s) d\mu(s) \\
&- \sum_{i \in D} \frac{1}{u_i(t)} \left(\sum_{r \in D} \int_{-h}^0 j_{i-r} u_r(t+s) \alpha_i(s) d\mu(s) + \sum_{r \in \mathbb{Z} \setminus D} \int_{-h}^0 j_{i-r} g_r(t+s) \alpha_i(s) d\mu(s) \right) \\
&\leq K_T + \sum_{i \in D} \sum_{r \in D} \int_{-h}^0 j_{i-r} u_r(t+s) \alpha_i(s) d\mu(s) - \sum_{i \in D} u_i(t),
\end{aligned}$$

where we have used that

$$\begin{aligned}
\sum_{i \in D} \frac{1}{u_i(t)} \left(\sum_{r \in D} \int_{-h}^0 j_{i-r} u_r(t+s) \alpha_i(s) d\mu(s) + \sum_{r \in \mathbb{Z} \setminus D} \int_{-h}^0 j_{i-r} g_r(t+s) \alpha_i(s) d\mu(s) \right) &\geq 0, \\
\sum_{i \in D} \sum_{r \in \mathbb{Z} \setminus D} \int_{-h}^0 j_{i-r} g_r(t+s) \alpha_i(s) d\mu(s) &\leq m C_T.
\end{aligned}$$

Integrating in (6) over $(\tau, \tau_k \wedge T)$ and taking expectations we obtain that

$$\begin{aligned}
0 &\leq \mathbb{E} V(u(\tau_k \wedge T)) \\
&\leq V(\phi(0)) + \mathbb{E} \int_{\tau}^{\tau_k \wedge T} K_T dt + \mathbb{E} \int_{\tau}^{\tau_k \wedge T} \sum_{i \in D} \left(1 - \frac{1}{u_i(t)}\right) b u_i(t) dw_i(t) \\
&+ \mathbb{E} \sum_{i \in D} \sum_{r \in D} \int_{-h}^0 \int_{\tau}^{\tau_k \wedge T} j_{i-r} u_r(t+s) \alpha_i(s) dt d\mu(s) - \mathbb{E} \sum_{i \in D} \int_{\tau}^{\tau_k \wedge T} u_i(t) dt.
\end{aligned}$$

Using $\bar{\alpha}_i \leq 1$ we have

$$\begin{aligned}
&\sum_{i \in D} \sum_{r \in D} \int_{-h}^0 \int_{\tau}^{\tau_k \wedge T} j_{i-r} u_r(t+s) \alpha_i(s) dt d\mu(s) \\
&= \sum_{i \in D} \sum_{r \in D} \int_{-h}^0 j_{i-r} \alpha_i(s) \int_{\tau}^{\tau_k \wedge T} u_r(t+s) dt d\mu(s) \\
&\leq \sum_{r \in D} \sum_{i \in D} j_{i-r} \int_{-h}^0 \alpha_i(s) d\mu(s) \int_{\tau-h}^{\tau_k \wedge T} u_r(t) dt \\
&\leq \sum_{r \in D} \int_{\tau-h}^{\tau_k \wedge T} u_r(t) dt = \sum_{r \in D} \int_{\tau}^{\tau_k \wedge T} u_r(t) dt + \sum_{r \in D} \int_{\tau-h}^{\tau} u_r(t) dt.
\end{aligned}$$

Hence,

$$\begin{aligned}
0 &\leq \mathbb{E}V(u(\tau_k \wedge T)) \\
&\leq V(\phi(0)) + K_T \mathbb{E}(\tau_k \wedge T) + \sum_{r \in D} \int_{\tau-h}^{\tau} \phi(t) dt \\
&\leq V(\phi(0)) + K_T T + K_\phi.
\end{aligned}$$

Let $\Omega_k = \{\omega : \tau_k \leq T\}$, which satisfies $P(\Omega_k) \geq \varepsilon$ for $k \geq k_1$. For any $\omega \in \Omega_k$ there is $i \in D$ such that either $u_i(\tau_k, \omega) = k$ or $u_i(\tau_k, \omega) = 1/k$, which implies that

$$V(u(\tau_k \wedge T, \omega)) \geq (k - 1 - \log(k)) \wedge \left(\frac{1}{k} - 1 + \log(k)\right).$$

Hence,

$$V(\phi(0)) + K_T T + K_\phi \geq \mathbb{E}(1_{\Omega_k} V(u(\tau_k \wedge T))) \geq \varepsilon((k - 1 - \log(k)) \wedge \left(\frac{1}{k} - 1 + \log(k)\right)) = \varepsilon R(k),$$

where 1_A stands for the indicator function of the set A . Passing to the limit as $k \rightarrow +\infty$ we obtain a contradiction as $R(k) \rightarrow +\infty$. ■

As a consequence, the following result follows.

Corollary 2 *Let $\phi^1, \phi^2 \in C([-h, 0], \mathbb{R}_+^m)$ be two initial conditions satisfying $\phi_i^1(s) > \phi_i^2(s)$ for any $i \in D$, $s \in [-h, 0]$. Also, $g^1, g^2 \in C([0, +\infty), l_2^\infty)$ are such that $g_i^1(t) \geq g_i^2(t)$ for all $i \in D$ and $t \geq \tau$. Then, $u_i(t) > v_i(t)$, for all $i \in D$ and $t \geq \tau$, where $u(\cdot), v(\cdot)$ are the unique solutions to problem (4) corresponding to $\{\phi^1, g^1\}$ and $\{\phi^2, g^2\}$, respectively.*

4 The non-linear case

Let us consider now the system

$$\begin{aligned}
\frac{d}{dt} u_i(t) &= [J(t, u_t)]_i - u^i(t) + b u_i(t)(1 - u_i(t)) \frac{dw_i}{dt}, \quad i \in D, t > \tau, \\
u^i(\tau + s) &\equiv \phi^i(s), \quad i \in D, s \in [-h, 0].
\end{aligned} \tag{7}$$

We are now interested in proving that the components of the solution remain in the interval $(0, 1)$ for every moment of time. In this way, we guarantee that the variables are probabilities if the initial conditions are as well.

Lemma 3 *Assume that $g_r(t) \in [0, 1]$, for all r and t , and that $\bar{\alpha}_i \leq 1$, for all i . Then, for any $\phi \in C([-h, 0], \mathbb{R}_+^m)$ such that $\phi_i(s) \in (0, 1)$, for any $i \in D$ and $s \in [-h, 0]$, the unique solution $u(\cdot)$ to (7) satisfies almost surely that $u_i(t) \in (0, 1)$ for all $i \in D$ and $t \geq \tau$.*

Proof. The existence and uniqueness of local solution is again guaranteed by [31, Theorem 2.8, P. 154]. Now we prove the statement of the Lemma.

Let $k_0 > 0$ be such that

$$\frac{1}{k_0} < \min_{s \in [-h, 0]} |\phi_i(s)| \leq \max_{s \in [-h, 0]} |\phi_i(s)| < k_0 \text{ for all } i \in D.$$

We define now the stopping time

$$\tau_k = \inf\{t \in [0, \infty) : u_i(t) \notin \left(\frac{1}{k}, 1 - \frac{1}{k}\right) \text{ for some } i \in D\}.$$

Since this sequence is increasing as $k \nearrow +\infty$, if $\tau_\infty = \lim_{k \rightarrow +\infty} \tau_k = +\infty$ a.s., then $0 < u_i(t) < 1$ almost sure for $t \geq 0$.

By contradiction, assume the existence of $T, \varepsilon > 0$ such that

$$P(\tau_\infty \leq T) > \varepsilon.$$

In such a case there would exist $k_1 \geq k_0$ such that

$$P(\tau_k \leq T) \geq \varepsilon \text{ for } k \geq k_1.$$

We denote

$$K_0 = \{u = (u_{m_1}, \dots, u_{m_2}) \in \mathbb{R}_+^m : 0 < u_i < 1\}$$

and define the C^2 -function $V : K_0 \rightarrow \mathbb{R}_+^1$ given by

$$V(u) = - \sum_{i \in D} (\log(1 - u_i) + \log(u_i)).$$

For $\tau \leq t \leq \tau_k \wedge T$ we have $u(t) \in K_0$, and then by Itô's formula we have

$$\begin{aligned} dV(u(t)) &= \sum_{i \in D} \left(\frac{1}{1 - u_i(t)} - \frac{1}{u_i} \right) \left(\sum_{r \in D} \int_{-h}^0 j_{i-r} u_r(t+s) \alpha_i(s) d\mu(s) + \sum_{r \in \mathbb{Z} \setminus D} \int_{-h}^0 j_{i-r} g_r(t+s) \alpha_i(s) d\mu(s) - u_i(t) \right) dt \\ &+ \sum_{i \in D} \frac{1}{2} \left(u_i^2(t) + (1 - u_i(t))^2 \right) b^2 dt + \sum_{i \in D} b(2u_i(t) - 1) dw_i(t) \\ &= I(t) dt + \sum_{i \in D} I_i(t) dw_i(t), \end{aligned}$$

where $I_i(t) = b(2u_i(t) - 1)$. First,

$$\sum_{i \in D} \left(-\frac{1}{u_i} \right) \left(\sum_{r \in D} j_{i-r} u_r(t) - u_i(t) + \sum_{r \in \mathbb{Z} \setminus D} j_{i-r} g_r(t) \right) \leq \sum_{i \in D} 1.$$

Second, by $\bar{\alpha}_i \leq 1$, $0 \leq g_r(t) \leq 1$ and (H2) we obtain that

$$\begin{aligned} &\sum_{r \in D} \int_{-h}^0 j_{i-r} u_r(t+s) \alpha_i(s) d\mu(s) + \sum_{r \in \mathbb{Z} \setminus D} \int_{-h}^0 j_{i-r} g_r(t+s) \alpha_i(s) d\mu(s) - u_i(t) \\ &\leq \sum_{r \in \mathbb{Z}} j_{i-r} \int_{-h}^0 \alpha_i(s) d\mu(s) - u_i(t) \\ &\leq 1 - u_i(t). \end{aligned}$$

Then the term $I(t)$ is estimated as follows:

$$I(t) \leq \sum_{i \in D} (2 + b^2) = m(2 + b^2).$$

Integrating over $(0, \tau_k \wedge T)$ and taking expectations we deduce that

$$\begin{aligned} 0 \leq \mathbb{E}V(u(\tau_k \wedge T)) &\leq V(\phi(0)) + \mathbb{E} \int_0^{\tau_k \wedge T} m(2 + b^2) dt + \mathbb{E} \int_0^{\tau_k \wedge T} \sum_{i \in D} b(2u_i(t) - 1) dw_i(t) \\ &= V(\phi(0)) + m(2 + b^2) \mathbb{E}(\tau_k \wedge T) \leq V(\phi(0)) + m(2 + b^2) T. \end{aligned}$$

Let $\Omega_k = \{\omega : \tau_k \leq T\}$, which satisfies $P(\Omega_k) \geq \varepsilon$ for $k \geq k_1$. For any $\omega \in \Omega_k$ there exists $i \in D$ such that either $u_i(\tau_k, \omega) = \frac{1}{k}$ or $u_i(\tau_k, \omega) = 1 - \frac{1}{k}$, so that

$$V(u(\tau_k \wedge T, \omega)) \geq \log(k) - \log\left(1 - \frac{1}{k}\right).$$

Thus,

$$V(\phi(0)) + m(2 + b^2)T \geq \mathbb{E}(1_{\Omega_k} V(u(\tau_k \wedge T))) \geq \varepsilon \left(\log(k) - \log\left(1 - \frac{1}{k}\right) \right).$$

Passing to the limit as $k \rightarrow +\infty$ we arrive at a contradiction. ■

5 Asymptotic behaviour

If we consider model (4) in the deterministic and autonomous cases, that is, $b = 0$ and $g_r(t) \equiv g_r \in \mathbb{R}$, and assume that $\alpha_i(s) = \alpha(s)$, for all $i \in D$, then it is well known [35] that there exists a unique fixed point \bar{u} given by the solution of the system

$$-M_1 \sum_{r \in D} j_{i-r} u_r + u_i = M_1 \sum_{r \in \mathbb{Z} \setminus D} j_{i-r} g_r = b_i, \quad i \in D, \quad (8)$$

where $M_1 = M_1(h) := \int_{-h}^0 \alpha(s) d\mu(s)$, provided that

$$M_1 \sum_{r \in D} j_{i-r} < 1 \quad \forall i \in D. \quad (9)$$

Moreover, $\bar{u}_r \geq 0$ for any $r \in D$ (see Remark 3.1 in [7]).

We will show that the solutions of the stochastic system remain close to this fixed point for large times in a suitable sense.

We start with the linear case.

Theorem 4 *Assume that $g_r \geq 0$, for all $r \in D$, $b < 1$ and that*

$$M_1(h) \sum_{r \in D} j_{i-r} < 1 - b^2 \quad \forall i \in D, \quad (10)$$

$$h < \frac{1}{2(1-b^2)} \log \left(\frac{1-b^2}{1-\delta(h)-b^2} \right), \quad (11)$$

where

$$\delta(h) = \min_{i \in D} \left\{ 1 - b^2 - M_1(h) \sum_{r \in D} j_{i-r} \right\}$$

Then, for any $\phi \in C([-h, 0], \mathbb{R}_+^m)$, the unique solution to problem (5) satisfies

$$\lim_{t \rightarrow +\infty} \sup \frac{1}{t} \int_0^t \sup_{\theta \in [-h, 0]} \mathbb{E}(\|u(s + \theta) - \bar{u}\|_{\mathbb{R}^m}^2) ds \leq \frac{2b^2 \|\bar{u}\|_{\mathbb{R}^m}^2}{\lambda^* - L(h, \lambda^*)},$$

where $L = L(h, \lambda) := 2(1 - \delta(h) - b^2)e^{\lambda h}$ and $\lambda^* \in (0, 2(1 - b^2))$ is such that $\lambda^* > L(h, \lambda^*)$.

Remark 5 *It is easy to see that (11) is satisfied for h small enough. Indeed, let h_0 be such that (10) holds for all $h \leq h_0$. If $h < h_0$ is small enough such that $h < \frac{1}{2(1-b^2)} \log \left(\frac{1-b^2}{1-\delta(h_0)-b^2} \right)$, the fact that $\delta(h)$ is non-increasing implies that $h < \frac{1}{2(1-b^2)} \log \left(\frac{1-b^2}{1-\delta(h)-b^2} \right)$.*

Remark 6 *Let $f(\lambda) = 2(1 - \delta(h) - b^2)e^{\lambda h} - \lambda$. Condition (11) implies that $f(2(1 - b^2)) < 0$. Then choosing λ^* close enough to $2(1 - b^2)$ we have that $f(\lambda^*) < 0$, so $\lambda^* > L(h, \lambda^*)$.*

Proof. We define the C^2 function $V : \mathbb{R}^m \rightarrow \mathbb{R}$ by

$$V(u) = \sum_{i \in D} (u_i - \bar{u}_i)^2 = \|u - \bar{u}\|_{\mathbb{R}^m}^2.$$

For $\lambda \in (0, 2(1 - b^2))$ we have

$$d(e^{\lambda t} V(u(t))) = \lambda e^{\lambda t} V(u(t)) dt + e^{\lambda t} dV(u(t))$$

and using Ito's formula we obtain that

$$\begin{aligned} dV(u(t)) &= \sum_{i \in D} 2(u_i - \bar{u}_i) \left(\sum_{r \in D} \int_{-h}^0 j_{i-r} u_r(t+s) \alpha(s) d\mu(s) + \sum_{r \in \mathbb{Z} \setminus D} \int_{-h}^0 j_{i-r} g_r \alpha(s) d\mu(s) - u_i(t) \right) dt \\ &\quad + \sum_{i \in D} u_i^2(t) b^2 dt + \sum_{i \in D} 2b(u_i(t) - \bar{u}_i) u_i(t) dw_i(t) \\ &= I(t) dt + \sum_{i \in D} I_i(t) dw_i(t). \end{aligned}$$

Using (8) the term $I(t)$ is estimated by

$$\begin{aligned} I(t) &= \sum_{i \in D} 2(u_i - \bar{u}_i) \left(\sum_{r \in D} \int_{-h}^0 j_{i-r} u_r(t+s) \alpha(s) d\mu(s) + M_1 \sum_{r \in \mathbb{Z} \setminus D} j_{i-r} g_r - u_i(t) \right) + \sum_{i \in D} u_i^2(t) b^2 \\ &\leq \sum_{i \in D} 2(u_i - \bar{u}_i) \left(\sum_{r \in D} \int_{-h}^0 j_{i-r} (u_r(t+s) - \bar{u}_r) \alpha(s) d\mu(s) - (u_i(t) - \bar{u}_i) \right) + 2b^2 \|u - \bar{u}\|_{\mathbb{R}^m}^2 + 2b^2 \|\bar{u}\|_{\mathbb{R}^m}^2 \\ &= \sum_{i \in D} 2(u_i - \bar{u}_i) \sum_{r \in D} \int_{-h}^0 j_{i-r} (u_r(t+s) - \bar{u}_r) \alpha(s) d\mu(s) - 2(1 - b^2) \|u - \bar{u}\|_{\mathbb{R}^m}^2 + 2b^2 \|\bar{u}\|_{\mathbb{R}^m}^2 \\ &= I_1(t) + I_2(t). \end{aligned}$$

Using the definition of $\delta(h)$ the first term is estimated by

$$\begin{aligned} I_1(t) &\leq M_1(h) \sum_{i \in D} (u_i(t) - \bar{u}_i)^2 \sum_{r \in D} j_{i-r} + \sum_{i \in D} \sum_{r \in D} \int_{-h}^0 j_{i-r} (u_r(t+s) - \bar{u}_r)^2 \alpha(s) d\mu(s) \\ &\leq (1 - \delta(h) - b^2) \sum_{i \in D} (u_i(t) - \bar{u}_i)^2 + \frac{(1 - \delta(h) - b^2)}{M_1(h)} \int_{-h}^0 \sum_{r \in D} (u_r(t+s) - \bar{u}_r)^2 \alpha(s) d\mu(s). \end{aligned}$$

Hence,

$$\begin{aligned} d(e^{\lambda t} V(u(t))) &\leq \lambda e^{\lambda t} \|u(t) - \bar{u}\|_{\mathbb{R}^m}^2 - 2(1 - b^2) \|u - \bar{u}\|_{\mathbb{R}^m}^2 e^{\lambda t} + 2b^2 \|\bar{u}\|_{\mathbb{R}^m}^2 e^{\lambda t} + (1 - \delta(h) - b^2) \|u(t) - \bar{u}\|_{\mathbb{R}^m}^2 e^{\lambda t} \\ &\quad + \frac{(1 - \delta(h) - b^2)}{M_1(h)} e^{\lambda t} \int_{-h}^0 \sum_{r \in D} (u_r(t+s) - \bar{u}_r)^2 \alpha(s) d\mu(s) + e^{\lambda t} \sum_{i \in D} I_i(t) dw_i(t). \end{aligned}$$

Integrating over $(0, t)$ and taking into account that $\lambda < 2(1 - b^2)$, we can discard the first two terms appearing on the right-hand side and deduce

$$\begin{aligned} e^{\lambda t} V(u(t)) &\leq V(u(0)) + \frac{2b^2 \|\bar{u}\|_{\mathbb{R}^m}^2}{\lambda} e^{\lambda t} + (1 - \delta(h) - b^2) \int_0^t \|u(s) - \bar{u}\|_{\mathbb{R}^m}^2 e^{\lambda s} ds \\ &\quad + \frac{(1 - \delta(h) - b^2)}{M_1(h)} \int_0^t e^{\lambda l} \int_{-h}^0 \sum_{r \in D} (u_r(l+s) - \bar{u}_r)^2 \alpha(s) d\mu(s) dl + \int_0^t e^{\lambda s} \sum_{i \in D} I_i(s) dw_i(s). \end{aligned}$$

Taking expectations we obtain

$$\begin{aligned}
e^{\lambda t} \mathbb{E} \|u(t) - \bar{u}\|_{\mathbb{R}^m}^2 &\leq \mathbb{E} \|u(0) - \bar{u}\|_{\mathbb{R}^m}^2 + \frac{2b^2 \|\bar{u}\|_{\mathbb{R}^m}^2}{\lambda} e^{\lambda t} + (1 - \delta(h) - b^2) \int_0^t \mathbb{E} \|u(s) - \bar{u}\|_{\mathbb{R}^m}^2 e^{\lambda s} ds \\
&\quad + \frac{(1 - \delta(h) - b^2)}{M_1(h)} \int_0^t e^{\lambda l} \int_{-h}^0 \mathbb{E} \|u(l+s) - \bar{u}\|_{\mathbb{R}^m}^2 \alpha(s) d\mu(s) dl \\
&\leq \mathbb{E} \|u(0) - \bar{u}\|_{\mathbb{R}^m}^2 + \frac{2b^2 \|\bar{u}\|_{\mathbb{R}^m}^2}{\lambda} e^{\lambda t} + (1 - \delta(h) - b^2) \int_0^t \mathbb{E} \|u(s) - \bar{u}\|_{\mathbb{R}^m}^2 e^{\lambda s} ds \\
&\quad + (1 - \delta(h) - b^2) \int_0^t \sup_{s \in [-h, 0]} \mathbb{E} \|u(l+s) - \bar{u}\|_{\mathbb{R}^m}^2 e^{\lambda l} dl \\
&\leq \mathbb{E} \|u(0) - \bar{u}\|_{\mathbb{R}^m}^2 + \frac{2b^2 \|\bar{u}\|_{\mathbb{R}^m}^2}{\lambda} e^{\lambda t} + 2(1 - \delta(h) - b^2) \int_0^t \sup_{s \in [-h, 0]} \mathbb{E} \|u(l+s) - \bar{u}\|_{\mathbb{R}^m}^2 e^{\lambda l} dl.
\end{aligned}$$

Notice that the last term makes sense thanks to [31, Lemma 2.3, P. 150], since this implies that $u \in L^2(\Omega; C([-h, T]; \mathbb{R}^m)) \subset C([-h, T], L^2(\Omega; \mathbb{R}^m))$.

We next replace t by $t + \theta$, $\theta \in [-h, 0]$, $t + \theta \geq 0$, in the above inequality. Then

$$\begin{aligned}
&\mathbb{E} \|u(t + \theta) - \bar{u}\|_{\mathbb{R}^m}^2 \\
&\leq e^{-\lambda(t+\theta)} \mathbb{E} \|u(0) - \bar{u}\|_{\mathbb{R}^m}^2 + \frac{2b^2 \|\bar{u}\|_{\mathbb{R}^m}^2}{\lambda} + 2(1 - \delta(h) - b^2) e^{-\lambda(t+\theta)} \int_0^{t+\theta} \sup_{s \in [-h, 0]} \mathbb{E} \|u(l+s) - \bar{u}\|_{\mathbb{R}^m}^2 e^{\lambda l} dl \\
&\leq e^{-\lambda t} e^{\lambda h} \mathbb{E} \|u(0) - \bar{u}\|_{\mathbb{R}^m}^2 + \frac{2b^2 \|\bar{u}\|_{\mathbb{R}^m}^2}{\lambda} + 2(1 - \delta(h) - b^2) e^{-\lambda t} e^{\lambda h} \int_0^t \sup_{s \in [-h, 0]} \mathbb{E} \|u(l+s) - \bar{u}\|_{\mathbb{R}^m}^2 e^{\lambda l} dl.
\end{aligned}$$

For $t + \theta < 0$ we have

$$e^{\lambda t} \mathbb{E} \|u(t + \theta) - \bar{u}\|_{\mathbb{R}^m}^2 \leq e^{\lambda t} \sup_{\theta \in [-h, 0]} \mathbb{E} \|u(\theta) - \bar{u}\|_{\mathbb{R}^m}^2 \leq e^{\lambda h} \sup_{\theta \in [-h, 0]} \mathbb{E} \|u(\theta) - \bar{u}\|_{\mathbb{R}^m}^2.$$

Thus, if we define the function

$$y(t) = \sup_{\theta \in [-h, 0]} \mathbb{E} \|u(t + \theta) - \bar{u}\|_{\mathbb{R}^m}^2,$$

then

$$e^{\lambda t} y(t) \leq y(0) e^{\lambda h} + \frac{2b^2 \|\bar{u}\|_{\mathbb{R}^m}^2}{\lambda} e^{\lambda t} + L(h) \int_0^t y(l) e^{\lambda l} dl$$

and Gronwall's lemma implies

$$\begin{aligned}
e^{\lambda t} y(t) &\leq y(0) e^{\lambda h} + \frac{2b^2 \|\bar{u}\|_{\mathbb{R}^m}^2}{\lambda} e^{\lambda t} + L(h) \int_0^t \left(y(0) e^{\lambda h} + \frac{2b^2 \|\bar{u}\|_{\mathbb{R}^m}^2}{\lambda} e^{\lambda h} e^{\lambda l} \right) e^{L(h)(t-l)} dl \\
&\leq y(0) e^{\lambda h} + y(0) e^{\lambda h} (e^{L(h)t} - 1) + \frac{2b^2 \|\bar{u}\|_{\mathbb{R}^m}^2}{\lambda} e^{\lambda t} + \frac{2b^2 \|\bar{u}\|_{\mathbb{R}^m}^2}{\lambda} e^{\lambda h} \frac{L(h)}{\lambda - L(h)} e^{L(h)t} (e^{(\lambda - L(h))t} - 1) \\
&\leq y(0) e^{\lambda h} e^{L(h)t} + \frac{2b^2 \|\bar{u}\|_{\mathbb{R}^m}^2}{\lambda - L(h)} e^{\lambda t},
\end{aligned}$$

and, consequently,

$$y(t) \leq y(0) e^{\lambda h} e^{(L(h) - \lambda)t} + \frac{2b^2 \|\bar{u}\|_{\mathbb{R}^m}^2}{\lambda - L(h)}.$$

Integrating over $(0, t)$ we have

$$\begin{aligned}
\frac{1}{t} \int_0^t y(s) ds &\leq \frac{y(0) e^{\lambda h}}{\lambda - L(h)} \frac{1 - e^{(L(h) - \lambda)t}}{t} + \frac{2b^2 \|\bar{u}\|_{\mathbb{R}^m}^2}{\lambda - L(h)} \\
&\leq \frac{y(0) e^{\lambda h}}{\lambda - L(h)} \frac{1}{t} + \frac{2b^2 \|\bar{u}\|_{\mathbb{R}^m}^2}{\lambda - L(h)}.
\end{aligned}$$

Therefore,

$$\limsup_{t \rightarrow +\infty} \frac{1}{t} \int_0^t y(s) ds \leq \frac{2b^2 \|\bar{u}\|_{\mathbb{R}^m}^2}{\lambda - L(h)},$$

which is true when $\lambda > L(h)$. Thus, the statement is proved. ■

Let us consider now system (7).

Theorem 7 Assume that $g_r \in [0, 1]$, for all $r \in D$, $b < 1$ and that (10), (11) hold. Then for any $\phi \in C([-h, 0], \mathbb{R}_+^m)$ such that $\phi_i(s) \in (0, 1)$, for all $i \in D$ and $s \in [-h, 0]$, the unique solution to problem (7) satisfies

$$\limsup_{t \rightarrow +\infty} \frac{1}{t} \int_0^t \sup_{\theta \in [-h, 0]} \mathbb{E}(\|u(s + \theta) - \bar{u}\|_{\mathbb{R}^m}^2) ds \leq \frac{2b^2 \|\bar{u}\|_{\mathbb{R}^m}^2}{\lambda^* - L(h, \lambda^*)},$$

where $L = L(h, \lambda) := 2(1 - \delta(h) - b^2)e^{\lambda h}$ and $\lambda^* \in (0, 2(1 - b^2))$ is such that $\lambda^* > L(h, \lambda^*)$.

Proof. As before, we define the C^2 -function $V : \mathbb{R}^m \rightarrow \mathbb{R}$ given by

$$V(u) = \sum_{i \in D} (u_i - \bar{u}_i)^2 = \|u - \bar{u}\|_{\mathbb{R}^m}^2.$$

For $\lambda \in (0, 2(1 - b^2))$ we have

$$d(e^{\lambda t} V(u(t))) = \lambda e^{\lambda t} V(u(t)) + e^{\lambda t} dV(u(t)).$$

Then, Ito's formula yields

$$\begin{aligned} dV(u(t)) &= \sum_{i \in D} 2(u_i - \bar{u}_i) \left(\sum_{r \in D} \int_{-h}^0 j_{i-r} u_r(t+s) \alpha(s) d\mu(s) + \sum_{r \in \mathbb{Z} \setminus D} \int_{-h}^0 j_{i-r} g_r \alpha(s) d\mu(s) - u_i(t) \right) \\ &\quad + \sum_{i \in D} u_i^2(t) (1 - u_i(t)^2 b^2) dt + \sum_{i \in D} 2b(u_i(t) - \bar{u}_i) u_i(t) (1 - u_i(t)) dw_i(t) \\ &= I(t) dt + \sum_{i \in D} I_i(t) dw_i(t). \end{aligned}$$

Since $\sum_{i \in D} u_i^2(t) (1 - u_i(t)^2 b^2) \leq \sum_{i \in D} u_i^2(t) b^2$, repeating the same steps in the proof of Theorem 4 we derive

$$\begin{aligned} e^{\lambda t} V(u(t)) &\leq V(u(0)) + \frac{2b^2 \|\bar{u}\|_{\mathbb{R}^m}^2}{\lambda} e^{\lambda t} + (1 - \delta(h) - b^2) \int_0^t \|u(s) - \bar{u}\|_{\mathbb{R}^m}^2 e^{\lambda s} ds \\ &\quad + \frac{(1 - \delta(h) - b^2)}{M_1(h)} \int_0^t e^{\lambda l} \int_{-h}^0 \sum_{r \in D} (u_r(l+s) - \bar{u}_r)^2 \alpha(s) d\mu(s) dl + \int_0^t e^{\lambda s} \sum_{i \in D} I_i(s) dw_i(s) \end{aligned}$$

and, taking expectations, we infer

$$e^{\lambda t} \mathbb{E} \|u(t) - \bar{u}\|_{\mathbb{R}^m}^2 \leq \mathbb{E} \|u(0) - \bar{u}\|_{\mathbb{R}^m}^2 + \frac{2b^2 \|\bar{u}\|_{\mathbb{R}^m}^2}{\lambda} e^{\lambda t} + 2(1 - \delta(h) - b^2) \int_0^t \sup_{s \in [-h, 0]} \mathbb{E} \|u(l+s) - \bar{u}\|_{\mathbb{R}^m}^2 e^{\lambda l} dl.$$

Again, the last term in the previous equation is well defined thanks [31, Lemma 2.3, P. 150]. Notice that as the solutions belong to $(0, 1)$ almost surely, the term in front of the noise has sub-linear growth Lemma 2.3 in [31] can be applied to this nonlinear case. The rest of the proof repeats the same argument as in Theorem 4. ■

6 Application to Life Tables

In this section, we will apply model (7) to predict the probability of death by age in Spain.

6.1 Life Tables: mortality modeling through a stochastic delay approach

Life tables are among the most widely used tools for studying survival and mortality patterns in a population. In demography, for instance, mortality constitutes one of the terms of the component method ([18], [26]) used for population estimates. In actuarial science, particularly in insurance applications, life tables are a fundamental tool for calculating, for example, adverse scenarios that insurance companies must be prepared to face.

These tables are structured around interrelated biometric functions (see, for example, [11], [4], [2]). Among these functions, we can highlight the probability of surviving to a completed age x , p_x ; its complement, the probability of death, q_x ; life expectancy at age x , e_x ; and the central death rate by age, m_x .

In practice, the true values of these functions are generally unknown and must be estimated from observed data. This estimation process can be approached from different methodological perspectives, typically grouped into three main categories: (i) stochastic versus non-stochastic models, (ii) parametric versus non-parametric models, and (iii) static versus dynamic approaches. Each of these axes defines key aspects in the modeling process: whether randomness is considered, whether structured functional forms are imposed, and whether the temporal evolution of mortality is incorporated.

Traditionally, the estimation of age-specific death probabilities (q_x) has been performed using data from a single time period. This procedure generates so-called crude death rates, which may lack desirable smoothness properties, such as the expected continuity between adjacent ages. To correct these irregularities, classical laws such as Gompertz's law [20], Gompertz-Makeham's law [30], or the Heligman-Pollard model [23], among others, have been proposed.

However, these approaches generally adopt a parametric and static perspective, in which the function q_x^t is assumed to remain constant over nearby time intervals. Nevertheless, it is well known that mortality rates evolve over time, meaning that assuming $q_x^t = q_x^{t+h}$ can lead to significant errors in many applications, such as pension expenditure projections or the calculation of technical reserves for insured portfolios. This realization has driven the development of dynamic mortality models, where the temporal evolution of q_x^t is modeled explicitly.

Among the best-known and most widely used dynamic models are the Lee-Carter models [29], the CBD model [8], and the extended M3–M7 family of models [9], [10]. These models introduce temporal improvement factors and stochastic components that capture the uncertainty associated with future mortality, offering interpretable structures and reasonable predictive performance.

In line with these models, in [34] a non-parametric dynamic model, based on kernel smoothing techniques to estimate mortality rates, was proposed. This model avoids rigid functional assumptions and uses a system of non-local differential equations to approximate the evolution of q_x^t over time. Although it successfully reproduces qualitative features of observed mortality, its predictive horizon is short (two to three years) due to the absence of historical information. To overcome this limitation, [35] proposed an improved model that incorporates past information through a delay term, specifically using mortality improvement rates [8]. This formulation retains the dynamic and non-parametric character of the original model while substantially enhancing its predictive capacity, extending its utility to time horizons of five to ten years. The underlying idea is that mortality trajectories are partially path-dependent, and thus the historical evolution must be considered.

This delay-based model remains within a non-stochastic framework, using observed improvement rates to incorporate past dynamics. It offers a robust alternative to stochastic models when precise deterministic prediction is required, as in regulatory contexts (e.g., Solvency II, [17]). However, despite its improved predictive performance, a major limitation persists: it does not offer 'alternative' mortality evolution scenarios, nor does it allow the calculation of quantiles or the construction of confidence intervals.

To address this issue, the non-local model proposed in [34] was extended into a stochastic model by introducing a random term into the original system of non-local differential equations. This extension aimed to capture both the temporal evolution and the intrinsic variability of the mortality phenomenon. The resulting model [7] strikes a compelling balance between interpretability, flexibility, and robustness, and aligns with the family of stochastic, non-parametric, and dynamic models (see [6], [14], [12]).

Despite providing a novel approach to integrating stochastic variability and non-parametric smoothing within a single mortality modeling framework, the need to incorporate historical information about mortality evolution became apparent. This leads to the model proposed in the present work, which can be classified as a dynamic, non-parametric, and stochastic model that also integrates historical information to capture

the temporal evolution of mortality.

6.2 Dynamical kernel graduation: combining stochastic behavior and historical data

The model proposed in equation (4) contains both delay and stochastic terms. In a similar way as in [35], in this work the delay term takes into account the history using the concept of *Improvement Rate* (see also [15], [21], [22] and [1]). These rates, denoted by $r_x^{t_0, t_1}$, treat to characterize the evolution of the mortality year-to-year or between two arbitrary moments, t_0 and t_1 , at a concrete age x ; they are defined by $r_x^{t_0, t_1} = q_x^{t_1} / q_x^{t_0}$. The difference $d = t_1 - t_0 > 0$ is the delay. Using these improvement rates, we define the *global improvement rate*, denoted by $\bar{r}_{t_0}^{t_1}$, as the coefficient of the linear model (without constant term) of the observed death rates, that is, we fit the linear model

$$q^{t_1} = \bar{r}_{t_0}^{t_1} \cdot q^{t_0}$$

with the data $\{q_0^{t_0}, \dots, q_\omega^{t_0}\}$ and $\{q_0^{t_1}, \dots, q_\omega^{t_1}\}$.

The procedure can be summarized as in ([35]):

1. We consider the observed mortality rates at each age (x) and each year (t): q_x^t , $x \in D = \{0, \dots, 100\}$, $t \in \{1908, \dots, 2018\}$. Also, we consider the values of $g_x(t)$, which is the rate of death either at "negative ages" or after the *actuarial infinite* (we have chosen it equal to 100).
2. We estimate the improvement rates for each age and delay, that is:

$\frac{year}{delay}$	1	2	3	4	...	109	110
$\bar{r}_{1908}^{1909} \sim \frac{q_{1908}^{1909}}{q_{1908}^{1908}}$	$\bar{r}_{1908}^{1910} \sim \frac{q_{1908}^{1910}}{q_{1908}^{1909}}$	$\bar{r}_{1908}^{1911} \sim \frac{q_{1908}^{1911}}{q_{1908}^{1910}}$	$\bar{r}_{1908}^{1912} \sim \frac{q_{1908}^{1912}}{q_{1908}^{1911}}$	$\bar{r}_{1908}^{1913} \sim \frac{q_{1908}^{1913}}{q_{1908}^{1912}}$	\dots	$\bar{r}_{1908}^{2017} \sim \frac{q_{1908}^{2017}}{q_{1908}^{2016}}$	$\bar{r}_{1908}^{2018} \sim \frac{q_{1908}^{2018}}{q_{1908}^{2017}}$
$\bar{r}_{1909}^{1910} \sim \frac{q_{1909}^{1910}}{q_{1909}^{1909}}$	$\bar{r}_{1909}^{1911} \sim \frac{q_{1909}^{1911}}{q_{1909}^{1910}}$	$\bar{r}_{1909}^{1912} \sim \frac{q_{1909}^{1912}}{q_{1909}^{1911}}$	$\bar{r}_{1909}^{1913} \sim \frac{q_{1909}^{1913}}{q_{1909}^{1912}}$	$\bar{r}_{1909}^{1914} \sim \frac{q_{1909}^{1914}}{q_{1909}^{1913}}$	\dots	$\bar{r}_{1909}^{2017} \sim \frac{q_{1909}^{2017}}{q_{1909}^{2016}}$	—
$\bar{r}_{1910}^{1911} \sim \frac{q_{1910}^{1911}}{q_{1910}^{1910}}$	$\bar{r}_{1910}^{1912} \sim \frac{q_{1910}^{1912}}{q_{1910}^{1911}}$	$\bar{r}_{1910}^{1913} \sim \frac{q_{1910}^{1913}}{q_{1910}^{1912}}$	$\bar{r}_{1910}^{1914} \sim \frac{q_{1910}^{1914}}{q_{1910}^{1913}}$	$\bar{r}_{1910}^{1915} \sim \frac{q_{1910}^{1915}}{q_{1910}^{1914}}$	\dots	—	—
$\bar{r}_{1911}^{1912} \sim \frac{q_{1911}^{1912}}{q_{1911}^{1911}}$	$\bar{r}_{1911}^{1913} \sim \frac{q_{1911}^{1913}}{q_{1911}^{1912}}$	$\bar{r}_{1911}^{1914} \sim \frac{q_{1911}^{1914}}{q_{1911}^{1913}}$	$\bar{r}_{1911}^{1915} \sim \frac{q_{1911}^{1915}}{q_{1911}^{1914}}$	\dots	\dots	—	—
\vdots	\vdots	\dots	—	—	—	—	—
$\bar{r}_{2016}^{2017} \sim \frac{q_{2016}^{2017}}{q_{2016}^{2016}}$	$\bar{r}_{2016}^{2018} \sim \frac{q_{2016}^{2018}}{q_{2016}^{2017}}$	—	—	—	—	—	—
$\bar{r}_{2017}^{2018} \sim \frac{q_{2017}^{2018}}{q_{2017}^{2017}}$	—	—	—	—	—	—	—

3. We consider the modified spheric function $\tilde{\gamma}$ given by

$$\tilde{\gamma}(s) = \begin{cases} T, & \text{if } s < b - a, \\ \gamma(b - s), & \text{if } b - a \leq s \leq b, \\ 0, & \text{if } s > b, \end{cases}$$

where

$$\gamma(s) = \begin{cases} \frac{T}{2} \left\{ 3\frac{s}{a} - \left(\frac{s}{a}\right)^3 \right\}, & \text{if } 0 \leq s \leq a, \\ T, & \text{if } s > a, \end{cases}$$

with $a = 20$, $b = 30$ and $T = 1$. We will use this function to calculate the annual improvement rates by delay, \bar{r}^d , which summarizes the previous information of the mortality process. We calculate a ponderated mean, with respect to the delay, of the improvement rates. For this aim, we define the vector $v = (v_i)$, $i = 1, \dots, n - 1$, $n = 111$, given by

$$v_i = \tilde{\gamma}(i).$$

Then, for each delay $d = 1, \dots, 110$, we define the vector $v^d = (v_i^d)$, $i = 1, \dots, n - d$, by

$$v_i^d = \frac{v_i}{\sum_{j=1}^{n-d} v_j},$$

and the

$$\bar{r}^d = \sum_{i=1}^{n-d} v_i^d \bar{r}_{\bar{t}+i}^{\bar{t}+i+d}, \quad (12)$$

being $\bar{t} = 1907$. In this way, the values $\bar{r}_{t_0}^{t_1}$ which are far enough from the present moment of time are not taken into account. We will refer to this values as the *global improvement rates for the delay d*.

4. Using the improvement rates by delay, \bar{r}^d , we define the function $\alpha(s)$ from (4), by putting

$$\alpha(-s) = 1 + \beta s, \quad s \in [0, h], \quad (13)$$

where β is the coefficient of the linear regression obtained from the data \bar{r}^d , $d = 1, 2, \dots, h$, and $h \leq 110$ is the maximum delay to be considered.

5. The experience of studying the mortality phenomenon allows us to assure that the importance of these rates are not the same for all delays. Indeed, the importance of the improvement rates increases when they are close to the time of prediction. To take this into account, we assume that the importance of these rates is modulated by a probability distribution function. To do this, we consider the exponential probability density function with the form

$$f_\lambda(s) = \begin{cases} \lambda e^{-\lambda s} & \text{if } s \geq 0, \\ 0 & \text{if } s < 0, \end{cases}$$

and obtain a density function in the interval $[0, h]$ by putting

$$\hat{f}_\lambda(s) = \frac{\lambda e^{-\lambda s}}{\int_0^h \lambda e^{-\lambda s} ds}, \quad s \in [0, h]. \quad (14)$$

Then we define the density function $\xi(\cdot)$ from (4) by $\xi(s) = \hat{f}_\lambda(-s)$ for $s \in [-h, 0]$.

In the particular case when in the numerical approximations we consider only integer delays, we can discretize the interval $[0, h]$ by using a finite number of integer delays $s = \{0, 1, \dots, d_{\max}\}$, where $d_{\max} = h \leq n - 1$, which is the maximum delay to be considered. Thus, instead of (14) we will use the discretized probability function

$$f^*(s) = \frac{\hat{f}_\lambda(s)}{\sum_{s=0}^{d_{\max}} \hat{f}_\lambda(s)}, \quad (15)$$

which approximates (14) at $s = 0, 1, \dots, d_{\max}$.

Using the annual improvement rates, and the exponential distribution, we can define the *weighted improvement rates* as

$$R_{weight}^d = \bar{r}^d \cdot f^*(d), \quad (16)$$

but they are not used in the numerical method.

In a similar way as in previous works (see [34], [35]), for each age x , for an arbitrary moment t and for a time step $\tau > 0$, the probability of death at $t + \tau$, denoted by $q_x(t + \tau)$, depends on:

- all graduate values at moment t , $q_z(t)$, $z \in D \subset \mathbb{Z}$ (via Gaussian kernel graduation, see [2]).
- all previous moments of time $t + s$, $s \in [-h, 0]$ (via improvement rates).

In the real world, when a phenomenon has a random nature, that is, there exists some kind of noise which can be intrinsic to the process under study, it is more suitable to introduce random fluctuations, for example to forecast adverse scenarios. Then, in this work, in a similar way as in [7], we introduce the stochastic term

$bq_i(t)(1 - q_i(t))\frac{dw_i}{dt}$ in the model, giving rise to equation (7). Applying the Euler-Maruyama discrete time approximation [28], the relation between $q_x(t + \tau)$ and $\{q_z(t)\}, \{q_z(t + s)\}_{s \in [-h, 0]}$ becomes:

$$\begin{aligned} q_x(t + \tau) &= \frac{1}{1 + \tau} q_x(t) + \frac{\tau}{1 + \tau} \sum_{z \in D} \int_{-h}^0 j_{x-z} q_z(t + s) \alpha(s) d\mu(s) \\ &+ \frac{\tau}{1 + \tau} \sum_{z \in \mathbb{Z} \setminus D} \int_{-h}^0 j_{x-z} g_z(t + s) \alpha(s) d\mu(s) + bq_x(t)(1 - q_x(t))(W_{x,t+\tau} - W_{x,t}), \end{aligned} \quad (17)$$

where j is a suitable kernel (in this work a Gaussian kernel), $g_z(\cdot)$ is the rate of death either at "negative ages" or after the *actuarial infinite*, $d\mu(s) = \hat{f}_\lambda(-s) ds$, where $\hat{f}_\lambda(-s), \alpha(s)$ are defined above. Relation (17) is consistent with the empirical experience on the actuarial practice.

In order to evaluate the integral $\int_{-h}^0 j_{x-z} g_z(t + s) \alpha(s) d\mu(s)$ we will use the classical Riemann sum with time step 1 and approximate the function $\hat{f}_\lambda(s)$ using the discretized probability function (15).

We observe that when the values $q_x(t)$ decrease over time, which is our case, the coefficient β in (13) is negative. Then

$$\bar{\alpha} = \int_{-h}^0 \alpha(s) \hat{f}_\lambda(s) ds = \int_{-h}^0 (1 - \beta s) \hat{f}_\lambda(s) ds = 1 - \beta \int_{-h}^0 s \hat{f}_\lambda(s) ds \leq 1,$$

so that assumption $\bar{\alpha} \leq 1$ is satisfied in Lemma 3.

6.3 Numerical simulation

We will implement our nonlinear stochastic model with delay (17) (NLSD for short) to predict the probability of death in Spain.

6.3.1 Data and parameters

The dataset used in this work has been obtained from [24]. The variables are the population and the central mortality rates for each age, which are taken from 0 to 100 years old (actuarial infinity). We use the observed values in Spain in the period 1908 – 2023.

The dataset has been splitted in two subsets. First, the period 1908 – 2018 is used to fit and calibrate the model; second, the period 2019 – 2023 is used for the validation of the model.

We have chosen the value $\lambda = \frac{11}{12}$ in the function (14).

The maximum delay h was set to 90. With this value, the estimated slope β is -0.003473 .

As a kernel we have chosen a discrete Gaussian Kernel with 0 mean, variance equal to 1 and bandwidth $b_w = 0.25$, which is defined as follows. We consider a finite set of ages $A = \{-m, -m + 1, \dots, x, \dots, M - 1, M\}$, where $0 \leq x \leq 100$, $m \geq 0$, $M \geq 100$. We define the set of distances

$$\mathbb{D}_x = \{d_{-m}, d_{-m+1}, \dots, d_0, d_1, \dots, d_M\} = \{x + m, x + m - 1, \dots, 1, 0, 1, \dots, M - x - 1, M - x\}.$$

Then, we define the truncated gaussian kernel $\hat{K}_b(\cdot)$ as

$$\hat{K}_b(k) = \frac{K_b(k)}{\sum_{\xi \in \mathbb{D}} K_b(\xi)}, \quad k \in \mathbb{D},$$

where $K(\cdot)$ denotes a density function from a standard gaussian random variable and $K_b(x) = \frac{1}{b_w} K(\frac{x}{b_w})$, $b_w = 0.25$.

In expression (17) we consider the truncated summatories with the restriction $-50 \leq z \leq 150$. Thus, we set $m = 50$, $M = 150$ for the discrete Gaussian kernel. In this way, for $x \in \{0, 1, \dots, 100\}$ we obtain:

$$j_{x-z} = \frac{K_b(|x - z|)}{\sum_{\xi \in \mathbb{D}_x} K_b(\xi)}, \quad \text{for } z \in \{-50, \dots, 150\},$$

where $\mathbb{D}_x = \{x + 50, \dots, 150 - x\}$.

Related with *actuarial infinity* (100 years old), the values of g_x for $x > 100$ are taken to be equal to 0.385, in a similar way as in [1]. For $x < 0$ the values of g_x^t are estimated using the expression $\frac{3}{4}q_0^t + \frac{1}{4}q_1^t$.

The proposed method enables forecasting over an arbitrary time horizon. Also, the method makes it possible to obtain several trajectories, that is, an ensemble of predictions. In particular, we have considered a time horizon of 15 years and a number of the trajectories equal to 500.

The time step τ in (17) is taken equal to 1. Although it is possible to use a smaller value for τ by interpolating the values of the variable in the past, the results are rather similar.

The increments $W_{x,t+\tau} - W_{x,t}$ are obtained using the Box-Muller algorithm [28], which gives a pair of pseudo-random numbers (z_1, z_2) that are independent and normally distributed with zero mean and variance equal to τ .

We have obtained the predicted trajectories for several values of the parameter b determining the intensity of the noise: $b = 0.1, 0.05$ and 0.025 .

6.3.2 Indicators

To validate the method and to determine if the proposed technique can be used in real applications, we define several indicators. These indicators, also, are used to compare different models. We consider two types of measures which can be classified as error, count and central measures.

Error measures. These measures compare the observed mortality rates with a synthetic trajectory. In this case, we use the *mean (or median) trajectory* of the realizations. Then, we calculate the *mean quadratic difference*, I_{MqD}^t , or the *mean relative quadratic difference*, I_{MRqD}^t , for each year. In particular we use the expressions

$$I_{MqD}^t = \frac{\sum_{x=0}^{100} (q_x^{t,obs} - \mathbb{E}(q_x^t))^2}{101} \text{ or } \chi_{MRqD}^t = \frac{\sum_{x=0}^{100} \frac{(q_x^{t,obs} - \mathbb{E}(q_x^t))^2}{\mathbb{E}(q_x^t)}}{101}. \quad (18)$$

Here, $q_x^{t,obs}$ are the observed rates to age x at time t , and $\mathbb{E}(q_x^t)$ are the mean value of the trajectories of the computed realizations.

Count measures. In the stochastic paradigm, it can be appropriate to use other indicators to determine if a method is good. The model proposed in this work, as well as other models which are used in the validation step, allows us to construct *synthetic empirical confidence intervals* $IC_{1-\alpha}$ with a given α level. Then, we define several indicators using these confidence intervals. In particular, we put

$$I_{c,1-\alpha}^t = \# \{x : q_x^{t,obs} \notin IC_{1-\alpha}\}. \quad (19)$$

For each year $I_{c,1-\alpha}^t$ summarizes the number of ages of the observed data at year t that do not belong to the α -synthetic confidence interval, $\alpha \in [0, 1]$. We will use $1 - \alpha = 0.98, 0.90$ and 0.80 .

Central measures and variability. It is important to point out that a stochastic model is suitable if it achieves a good balance between coverage and precision. For instance, if the confidence intervals are narrow but do not contain the observed (or future) values, such a model underestimates uncertainty and may lead to serious consequences—for example, if an insurance company fails to allocate sufficient capital reserves to meet future claims. On the other hand, if the resulting confidence intervals are too wide, even if they always include the observed or future values, the model overestimates uncertainty, thus losing predictive value and potentially causing significant harm—for example, by requiring capital to be reserved for specific purposes, thereby limiting its availability for others, such as healthcare or pensions. Hence, in the indicators of this type we take into account both the precision of the mean values and the dispersion of the realizations in order to compare the methods. Using the same notation as in (18) we define, in a similar way as in [13], the following indicator:

$$I_{CT,\tau}^t = \frac{\sum_{x=0}^{100} (q_x^{t,obs} - \mathbb{E}(q_x^t))^2}{(\sigma_x^t)^\tau}, \quad (20)$$

where σ_x^t is the standard deviation of the trajectories of the computed realizations to age x at time t and either $\tau = 1$ or $\tau = 2$.

6.3.3 Software

The software used to implement the numerical method has been MATLAB (versión R2024b).

The R-software ([36]) has been used to download the dataset from [24] (using package *demography*, [25]). Also, the R-software has been used to implement the models Lee-Carter, Renshaw-Haberman, CBD and the family M3-M7 using the package StMoMo ([37]); this package has been used to determine the best models. The R-software has been used to estimate the count, error and central measures used to validate our model and to determine which are the best models. The figures have been created using the R-software.

6.3.4 Numerical results

This section is dedicated to the validation of the proposed method and to compare it with others techniques.

In this first part, we show graphically how the NLSD method reproduces the qualitative behavior of the mortality curve. In the second part, we compare the NLSD method with the classical ones, in particular with the Lee-Carter and Renshaw-Haberman methods.

Figure 1 shows, for the year 2023, that the mean trajectory obtained by the NLSD method is closed to the observed rates. The same behavior can be verified for the rest of the years in the validation period (2019 – 2023). Also, qualitatively, we can observe how the mean realization reproduces the form of the mortality curve, with the usual parts: adaptation to the environment (ages 0-16), natural longevity (ages 16-100) and social jump (ages 16-27).

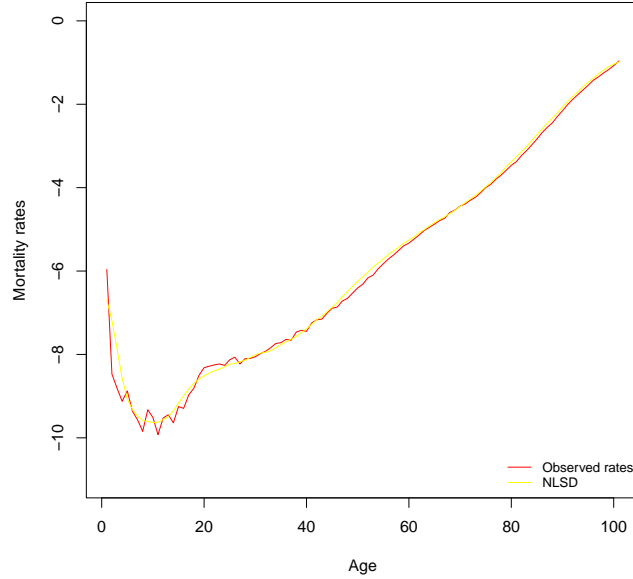
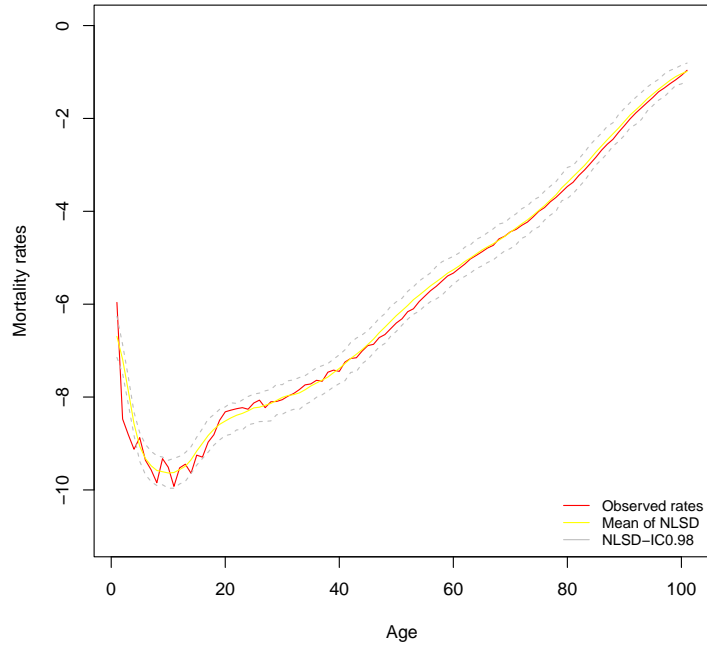
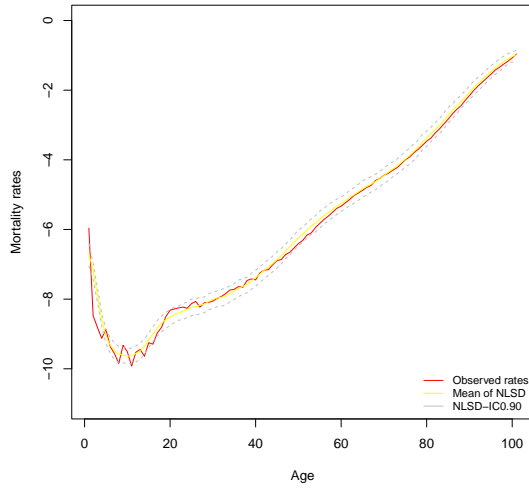


Figure 1: Mean trajectory: $b = 0.1$

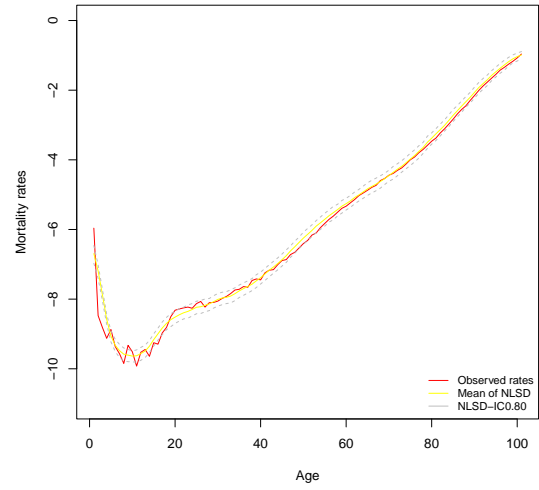
Figures 2a-2c and Figures 3a-3c show, for the 5-year horizon of forecasting, if the observed rates belong or not to the intervals $IC_{0.98}$, $IC_{0.90}$ and $IC_{0.80}$ for $b = 0.1$ and $b = 0.025$.



(a) Confidence Level: $1 - \alpha = 0.98$

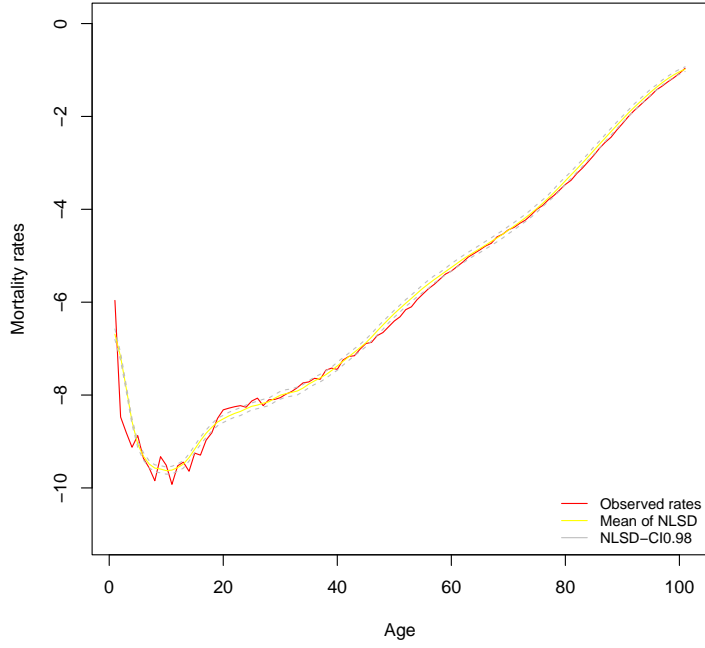


(b) Confidence Level: $1 - \alpha = 0.9$

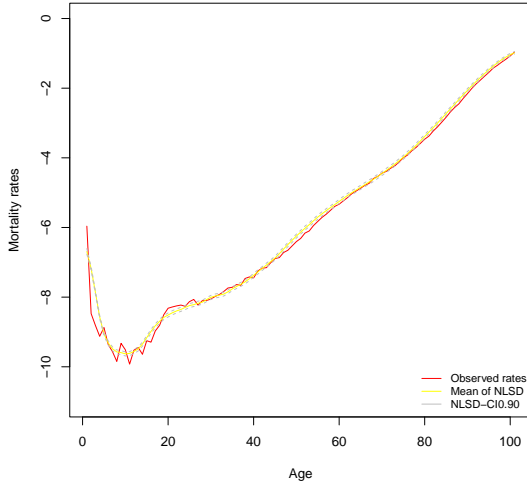


(c) Confidence Level: $1 - \alpha = 0.8$

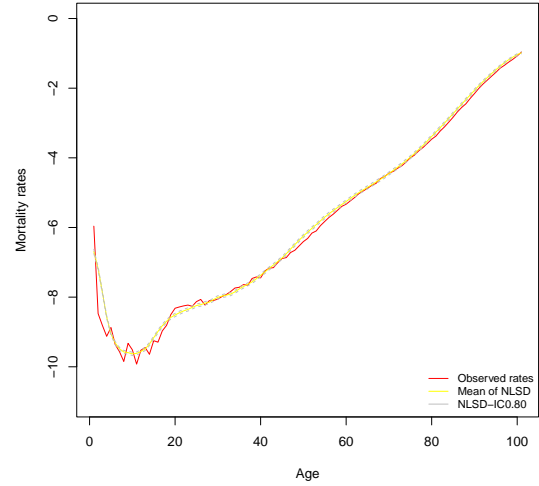
Figure 2: Confidence Intervals for several confidence levels ($b = 0.1$).



(a) Confidence Level: $1 - \alpha = 0.98$



(b) Confidence Level: $1 - \alpha = 0.9$



(c) Confidence Level: $1 - \alpha = 0.8$

Figure 3: Confidence Intervals for several confidence levels ($b = 0.025$).

In the context of real applications, forecasting several plausible scenarios often requires more than just the mean trajectory. For example, when the mortality rates are used as input data in nonlinear estimations, as in the calculation of the cost of claims using mechanisms based on compound interest rates, it becomes convenient to account for random fluctuations. As we can see in Figure 4, the proposed method allows us to estimate not only the mean trajectories but also an arbitrary number of equally probable realizations.

Further, with the aim of comparison, we apply different methods using the same data in the period

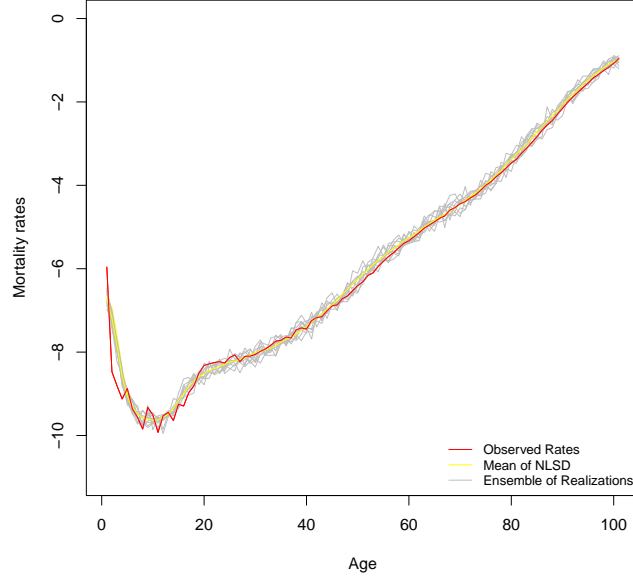


Figure 4: Ensemble of realizations: $b = 0.1$

1908-2018 and forecast the mortality rates for the period 2019-2023. Then, we calculate the indicators which have been defined previously.

As we said before, initially we have considered several methods such as the Lee-Carter (LC), Renshaw-Haberman (RH) and CBD methods, and the models M3-M7. With the aim of facilitating the interpretation of the results, we have selected the best-fitting methods. The selection is due using the Akaike Information Criterion (AIC) and the Bayesian Information Criterion (BIC). With these indicators, and using the package StMoMo in the R-software, it has been determined that the Renshaw-Haberman method and the Lee-Carter method are the most suitable.

Figure 5 shows us the results for the year 2023: the observed data and the mean value of the trajectories for each technique. In the NLSD method, $b = 0.1$.

Figure 5 provides evidence about the suitability of the proposed method. Even though the proposed technique seems to be, graphically, the better technique, it is important to note that none of the three evaluated techniques has been specifically calibrated, and the default parameter values of the StMoMo package have been used for the LC and RH methods.

Complementarily, we can use the quantitative measures to determine the goodness of each model and to compare them.

We start with the count indicators. Table 1 shows the number of ages (for each year into the period of the validation) that do not belong to the confidence interval, $IC_{0.98}$, and for each of the evaluated methods. Tables 2 and 3 show the same information for the confidence intervals $IC_{0.90}$ and $IC_{0.80}$. Our method has been tested with different values of the parameter b (0.1, 0.05 and 0.025), which determines the intensity of the noise.

Method\year	2019	2020	2021	2022	2023
NLSD 0.1	7	6	4	8	5
NLSD 0.05	17	56	21	18	33
NLSD 0.025	50	75	53	39	67
LC	65	80	70	63	71
RH	71	88	81	81	84

Table 1: $r_{c,0.98}^t$

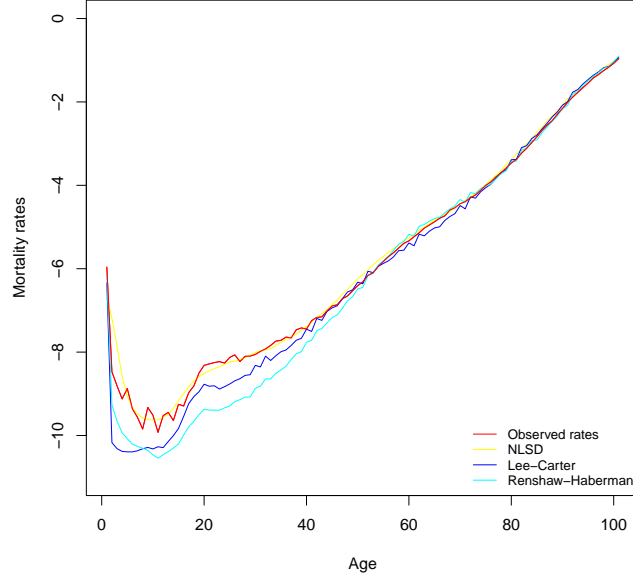


Figure 5: Mean trajectories

Method\year	2019	2020	2021	2022	2023
NLSD 0.1	10	18	9	11	16
NLSD 0.05	26	66	36	28	59
NLSD 0.025	64	84	66	50	82
LC	77	93	80	72	82
RH	78	93	82	87	87

Table 2: $I_{c,0.9}^t$

Method\year	2019	2020	2021	2022	2023
NLSD 0.1	15	44	17	15	28
NLSD 0.05	41	72	48	34	64
NLSD 0.025	72	91	75	67	86
LC	79	95	85	75	88
RH	85	94	89	91	91

Table 3: $I_{c,0.8}^t$

By analyzing the tables of the count-based indicators, we can conclude that the proposed technique captures the observed mortality more effectively. This suggests that, in this regard, it provides a better fit than the other approaches. However, this does not necessarily imply that the technique is more accurate, as the result may be due to a more conservative forecast, so we have to consider other indicators as well.

Complementary to the count-based indicators, error metrics may be useful for assessing whether the technique is as accurate as, or more or less accurate than, the LC and RH models. Using the indicators (18) over the full 0-100 age range we obtain the results in Tables 4 and 5.

Method\year	2019	2020	2021	2022	2023
NLSD 0.1	2.256290e-05	2.236960e-05	2.260896e-05	2.961290e-05	1.518093e-05
NLSD 0.05	1.103389e-04	1.091354e-04	1.090309e-04	1.070186e-04	1.554116e-04
NLSD 0.025	1.075917e-05	1.107349e-05	1.083946e-05	1.529299e-05	1.772229e-05
LC	3.135750e-05	3.088876e-05	3.099892e-05	2.791308e-05	4.069674e-05
RH	3.186545e-05	3.139071e-05	3.097631e-05	2.684819e-05	1.960841e-05

Table 4: I_{MqD}^t

Method\year	2019	2020	2021	2022	2023
NLSD 0.1	1.162379e-04	1.168913e-04	1.174218e-04	1.815611e-04	9.268740e-05
NLSD 0.05	4.740293e-04	4.682191e-04	4.692663e-04	4.908082e-04	7.605474e-04
NLSD 0.025	7.714122e-05	7.831104e-05	7.724071e-05	1.283547e-04	1.373643e-04
LC	1.075780e-04	1.061766e-04	1.066380e-04	1.506715e-04	2.467346e-04
RH	2.252991e-04	2.267182e-04	2.237182e-04	1.858389e-04	1.321769e-04

Table 5: I_{MRqD}^t

Tables 4 and 5 allow us to compare the methods. We have highlighted in bold the values with lowest error for each year. According to Table 4, the method NLSD has the lowest error accross all the years. In particular, NLSD with $b = 0.025$ outperforms both the LC and RH methods in all the years. In Table 5, NLSD (with $b = 0.025$) is the most accurate method in four out of five years, while RH performs best in one (although the error value for NLSD is nearly identical to that of RH in that case). The LC model does not achieve the lowest error in any of the five years for either indicator.

Central measures are also very useful to assess the accuracy of the methods. In Table 6 one can see the values of the indicators (20) in the year 2023.

	$I_{CT,1}^{2023}$	$I_{CT,2}^{2023}$
NLSD 0.1	0.18	149.54
NLSD 0.05	0.36	623.98
NLSD 0.025	0.70	<i>2490.81</i>
LC	0.88	2109.89
RH	1.74	103496.19

Table 6: $I_{CT,\tau}^t$

The indicator $I_{CT,1}^{2023}$ yields better results for NLSD across all three levels of noise intensity. The indicator $I_{CT,2}^{2023}$ is better for NLSD for $b = 1$ and $b = 0.05$, while LC slightly outperforms NLSD for $b = 0.025$. The values obtained for RH are significantly worse than for the other methods.

Figure 6 shows the estimated density functions for several ages and each method. From this picture we can see graphically the variability, which is different for each age and method. This change in variability from one technique to another, when directly comparing the estimated mean values and the observed values, highlights the importance of accounting for such variability in order to accurately assess the precision of each technique.

When $b = 0.025$, for most ages, the NLSD method yields mean values closest to the observed values, while maintaining a level of variability comparable to the other methods. At the oldest age (80), the LC method provides the best coverage, albeit at the cost of high variability in the realizations. Moreover, for younger and middle ages, the realizations from the LC method fail to cover the observed value, despite exhibiting greater variability.

We have seen that the NLSD method can be applied to real-world scenarios with high short-term accuracy. To assess whether this technique is also effective in the medium or long term, we examine whether its predicted values align with those obtained from the RH and LC methods. Figure 7 displays the mean prediction trajectories over a 10-year horizon (with predictions for 2028 based on observed data up to 2018).

We observe that the predicted values are similar in magnitude across the three techniques. However, there exist differences at the youngest and oldest ages. The predictions diverge most at the earliest ages, where the NLSD model produces the highest values, followed by LC with intermediate values, and RH with the lowest.

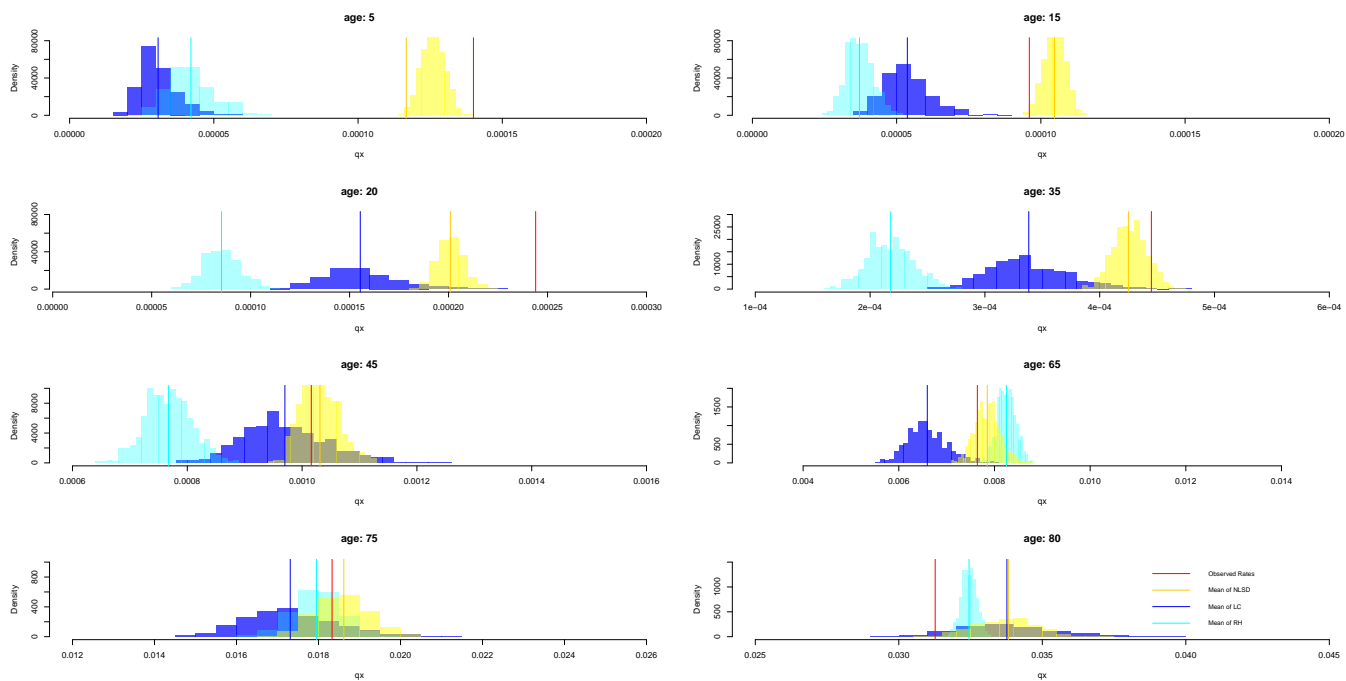


Figure 6: Density function, $b = 0.025$

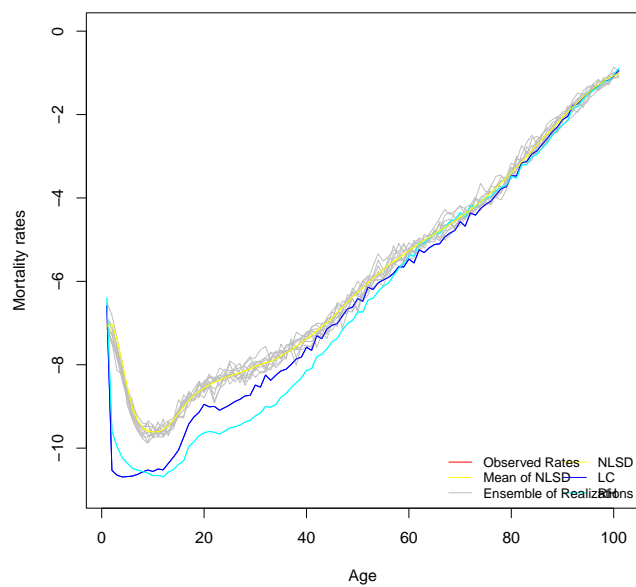


Figure 7: Mean trajectories

From a qualitative point of view, it is worth noting that the analysis of historical time series indicates a decreasing intensity of the social hump over time. In this regard, the NLSD model exhibits a more realistic behavior compared to the LC and RH models.

It is also important to highlight that the LC and RH models generate predictions using autoregressive and moving average time series models (ARIMA), which possess the following characteristics:

1. They make linear forecasts by extrapolating the dynamics of the most recent values. For instance, recent improvement in mortality rates may be projected forward, potentially leading to underestimations of future mortality levels.
2. They exhibit an *uncertainty cone* that grows rapidly so their predictive performance deteriorates significantly as the forecast horizon increases. In Economics, for example, it is common to use a 12-step monthly forecast horizon. For annual forecasts, typical horizons are 3, 5, or 7 years.

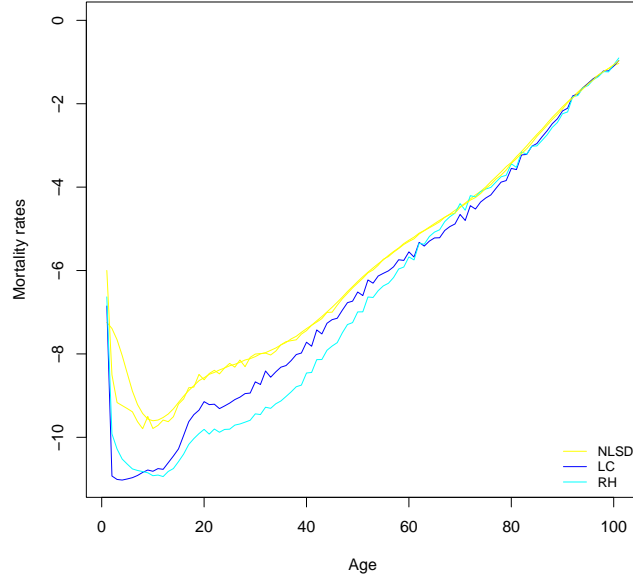


Figure 8: Mean trajectories

Figure 8 shows the predictions for the year 2033 (15-year horizon). This figure exhibits a similar pattern to that observed in the 10-year horizon, but the differences between the methods become more pronounced.

7 Conclusions

This work proposes a method for modeling and forecasting mortality rates. It constitutes an improvement over previous studies ([34], [35], [7]), by incorporating both the historical evolution of the mortality phenomenon and its random behavior.

The first part of the study introduces the NLSD model and analyzes mathematical properties such as the existence of solutions and their asymptotic behavior. The second part presents an application of the NLSD model. For this purpose, the Euler–Maruyama method is applied to data obtained from the Human Mortality Database [24]. The choice of the HMD is justified by the fact that it contains mortality datasets from a large number of countries, all of which have been methodologically harmonized. The use of Spanish data is arbitrary; the method has also been tested with data from other countries, such as the UK, although we do not show these results in this paper.

To assess the validity of the proposed method, the observation period was divided into two subsets: one for fitting and calibration (1908 – 2018), and another for validation (2019 – 2023).

The evaluation was carried out by comparing the proposed model with other widely used approaches, such as the LC, RH, CBD, and M3–M7 models. Count-based, error-based and central metrics were used in the comparison. The NLSM model achieved the best results for all years within the validation period.

Based on this study, we can conclude that the NLSM model should be regarded as a promising alternative to classical models. While a more exhaustive validation remains to be conducted, the method has shown the best performance among the models tested.

As extensions of this study, we propose conducting a sensitivity analysis of the parameters, as well as an exhaustive comparison across different regions and time periods. From a technical perspective, it would be valuable to incorporate optimization techniques for parameter estimation and to assess the applicability of cross-validation strategies.

Acknowledgements. The research has been partially supported by the Spanish Ministerio de Ciencia e Innovación (MCI), Agencia Estatal de Investigación (AEI) and Fondo Europeo de Desarrollo Regional (FEDER) under the project PID2021-122991NB-C21.

Conflict of interest. The authors declare that they do not have any conflict of interest.

References

- [1] I. Albarrán Lozano, F. Ariza Rodríguez, V.M. Cóbrecas Juárez, M.L. Durbán Reguera, J.M. Rodríguez-Pardo del Castillo, Riesgo de Longevidad y su aplicación práctica a Solven-
cia II. VIII International Awards "Julio Castelo Matrán", Fundación Mapfre. Available on-
line: https://www.fundacionmapfre.org/fundacion/es_es/publicaciones/diccionario-mapfre-seguros/r/riesgo-de-longevidad.jsp.
- [2] M. Ayuso, H. Corrales, M. Guillén, A.M. Perez-Marín, J.L. Rojo, *Estadística Actuarial Vida*, Universitat de Barcelona Edicions, Barcelona, 2007.
- [3] E. Barbi, F. Lagona, M. Marsili, J.W. Vaupel, W.W. Kenneth, The plateau of human mortality: de-
mography of longevity pioneers, *Science*, **360** (2018). 1459-1461.
- [4] B. Benjamin, J.H. Pollard, *The analysis of mortality and other actuarial statistics*, Institute of Actuaries and the Faculty of Actuaries, Oxford, 1993.
- [5] M. Bogoya, C.A Gómez S., Discrete model of a nonlocal diffusion equation, *Rev. Colombiana Mat.*, **47** (2013), 83–94.
- [6] N. Brouhns, M. Denuit, I.V. Keilegom, Bootstrapping the Poisson log-bilinear model for mortality forecasting, *Scand. Actuar. J.*, **3** (2005), 212-224.
- [7] T. Caraballo, F. Morillas, J. Valero, On a stochastic nonlocal system with discrete diffusion modeling life tables, *Stoch. Dyn.*, **22** (2022).
- [8] A.J.G. Cairns, D. Blake, K. Dowd, Modelling and management of mortality risk: a review. *Scandinavian Actuarial Journal* **2008** (2008) 79-113.
- [9] A.J.G. Cairns, D. Blake, K. Dowd, G.D. Coughlan, D. Epstein, M. Khalaf-Allah, Mortality density forecasts: an analysis of six stochastic mortality models, *Insurance Math. Econom.*, **48** (2011) 355-367.
- [10] A.J.G. Cairns, D. Blake, K. Dowd, G.D. Coughlan, D. Epstein, A. Ong and I.A. Balevich, Quantitative comparison of stochastic mortality models using data from England and Wales and the United Statesm, *N. Am. Actuar. J.*, **13** (2009) 1-35.
- [11] C.L. Chiang, *The life tables and its applications*, Krieger Publishing Company, Malabar, FL, USA, 1984.
- [12] J.B. Copas, S. Haberman Non-parametric graduation using kernel methods, *J. Inst. Actuaries*, **110** (1983) 135-156.

- [13] A.P. Dawid, P. Sebastiani, Coherent dispersion criteria for optimal experimental design, *The Annals of Statistics*, **27** (1999), 65-81. <https://doi.org/10.1214/aos/1018031108>.
- [14] E. Dodd, E., J.J. Forster, J. Bijak, P.W.F. Smith, Smoothing mortality data: Producing the English life table, 2010-12, *J. R. Stat. Soc. Ser. A Stat. Soc.*, **181** (2016), 1-19.
- [15] E. Dodd, E., J.J. Forster, J. Bijak, P.W.F. Smith, Stochastic modelling and projection of mortality improvements using a hybrid parametric/semi-parametric age-period-cohort model, *Scand. Actuar. J.*, 2021 (2), 134-155, DOI: 10.1080/03461238.2020.1815238.
- [16] E. Dolgin, Longevity data hint at no natural limit on lifespan, *Nature*, **559** (2018) 14-15.
- [17] European Parliament and of the Council, *Risk management and supervision of insurance companies* (Solvency II) - Consolidated text: Directive 2009/138/EC of the European Parliament and of the Council of 25 November 2009 on the taking-up and pursuit of the business of Insurance and Reinsurance. Available online: <https://eur-lex.europa.eu/> [on-line: 2020/12/6].
- [18] Eurostat, Population projections in the EU. Statistics Explained, 2024, March 4, <https://ec.europa.eu/eurostat/statistics-explained/index.php?oldid=596339> [29/04/2025].
- [19] J. Gavin, S. Haberman and R. Verrall, Graduation by Kernel and adaptive kernel methods with a boundary correction, *Transactions of the Society of Actuaries*, **XLVII** (1995) 1-37.
- [20] B. Gompertz, On the nature of the function of the law of human mortality and on a new mode of determining the value of life contingencies, *Transactions of The Royal Society*, **115** (1825) 513-585.
- [21] S. Haberman, A. Renshaw, Parametric mortality improvement rate modelling and projecting, *Insurance Math. Econom.*, **50** (2012), 309-333.
- [22] S. Haberman, A. Renshaw, Modelling and projecting mortality improvement rates using a cohort perspective, *Insurance Math. Econom.*, **53** (2013), 150-168.
- [23] L.M.A. Helligman, J.H. Pollard, The age pattern of mortality, *J. Inst. Actuaries*, **107** (1980) 49-82.
- [24] Human Mortality Database. Series of death rates of Spain, University of California, Berkeley (USA), and Max Planck Institute for Demographic Research (Germany). Available at www.mortality.org or www.humanmortality.de (data downloaded on [2025/04/15]).
- [25] R.J. Hyndman (with contributions by Heather Booth, Leonie Tickle and John Maindonald), Package demography: forecasting mortality, fertility, migration and population data (R package version 1.22), 2019, <https://CRAN.R-project.org/package=demography>.
- [26] Instituto Nacional de Estadística (INE), Metodología de las estimaciones intercensales de población, https://www.ine.es/inebaseDYN/ecp30282/docs/meto_estimaciones_pobla.pdf [29/04/2025].
- [27] Instituto Nacional de Estadística (INE), *Life tables: Methodology*.
- [28] P.E. Kloeden, E. Platen, H. Schurz, *Numerical Solution of SDE through Computer Experiments*, Springer, Berlin, 1994.
- [29] R. Lee, L. Carter, Modelling and forecasting US mortality, *J. Am. Stat. Assoc.*, **87** (1992), 659-671.
- [30] W. Makeham, On the law of mortality and the construction of annuity tables, *Journal of the Institute of Actuaries*, **8** (1869), 301-310.
- [31] X. Mao, *Stochastic Differential Equations and Applications*, Woodhead Publishing Limited, Cambridge, UK, 1997.
- [32] T. Missov, Gamma-Gompertz life expectancy at birth, *Demographic Research*, **28** (2013), 259-270.

- [33] F.G. Morillas, I.B. Sampere, Using wavelet techniques to approximate the subjacent risk of death, In *Modern Mathematics and Mechanics*, V.A. Sadovnichiy and M.Z. Zgurovsky eds. (Cham, Switzerland, Springer International Publishing, 2019), Chapter 28, pp. 541-557.
- [34] F. Morillas, J. Valero, On a nonlocal discrete diffusion system modeling life tables, *RACSAM*, **108** (2014), 935-955.
- [35] F. Morillas, J. Valero, On a retarded nonlocal ordinary differential system with discrete diffusion modeling life tables, *Mathematics*, *9* (2021), 220.
- [36] R Core Team, *R: a language and environment for statistical computing*, R Foundation for Statistical Computing, Vienna, Austria, 2020. Available online: <https://www.R-project.org/>.
- [37] A.M. Villegas, V.K. Kaishev, P. Millossovich, StMoMo: An R package for stochastic mortality modeling, *J. Stat. Software*, **84** (2018), 1-38.